PROPAGATION OF DETONATION WAVES IN RADIALLY GRADED EXPLOSIVES

R. Guirguis, A. Landsberg, H. Sandusky, and A. Wardlaw
Naval Surface Warfare Center
Indian Head, MD 20640-5035

The reaction zone of detonation waves propagating in radially graded explosives is resolved using both analytic techniques and numerical simulations. Unlike traditional waves, special detonations with highly curved fronts and/or incorporating regions of negative thermicity can steadily propagate in these explosives. As a result, the direction of the transverse pressure gradient is reversed. This can laterally drive the gas products from partially decomposed regions downstream back to the shock front where these hot gases can participate in igniting some of the yet unreacted material in the reaction zone instead of solely depending on the shock-induced hot spots, thus establish a convective detonation wave.

INTRODUCTION

Spatially graded explosives, usually abbreviated as gradient explosives, are charges in which the chemical and/or physical compositions gradually change from point to point. Layered explosives are made of layers of different compositions, but within each layer, the composition is uniform. The sudden jump in properties at the interface between adjacent layers can introduce strong reflection and refraction waves. In a gradient explosive the properties also change, but gradually, so the detonation is transmitted from point to point without introducing any appreciable reflection or refraction waves.

In general, introducing a gradient in the composition allows the formulator and warhead designer additional degrees of freedom beyond the scope of current, traditional uniform explosives. For example, by controlling the angle of inclination of the detonation front to the liner of a shaped charge, the velocity of the resulting jet can be enhanced. Detonations can be steadily propagated in gradient explosives smaller than the critical diameter of the corresponding charge containing on average the same components, but uniformly distributed. Corner turning effects can be eliminated by having the corners rich with an explosive material that can support a relatively faster detonation wave than the bulk of the charge.

This work was conducted under the auspices of the Core Research Program in NSWC, Indian Head.

In a previous paper[1] the mathematical aspects of modeling detonations in gradient explosives were introduced. The simulations showed that after a transitional zone, a detonation initiated in a radially graded charge reaches steady state, at which point, and except for those introduced by the interaction with the confinement, all pressure waves emanating from the front disappear. The results also showed that by controlling the distribution, the detonation can be shaped to form convex or concave fronts, and in both cases, highly curved detonations can be sustained (steadily propagated).

In another paper[2] the concept of convective detonations was introduced, which refers to special detonation waves in which convective burning plays a significant role in ignition, not unlike its role in deflagration-to-detonation transitions (DDT) often observed in porous propellants. Specifically, the hot decomposition products infiltrate upstream through the pores and drastically increase the flame speed beyond that of laminar propagation. A compression phase in which the flame-generated pressure waves coalesce ahead of the deflagration front always precedes the final stages of transition. In traditional detonations, however, the pressure gradient is always pointed downstream. Convective burning can participate in the surface decomposition stage of the reaction, but it cannot contribute to ignition. By definition, to establish a convective detonation, instead of solely depending on the shock-induced hot spots, convection of the

hot gas products has to significantly contribute to igniting the unreacted explosive coming through the front.

In reference 2 it was conjectured that convective detonations are possible in radially graded charges. Based on heuristic arguments it was speculated that in the highly curved detonations sustained in these explosives, the direction of the transverse pressure gradient (orthogonal to the streamlines) is reversed, such as to laterally drive some of the decomposition products back to the shock. In this paper 2 different techniques were used to demonstrate that in regions where the change in composition causes a local increase in the curvature of the front and/or negative thermicity, the direction of the transverse pressure gradient is indeed reversed. An analytical method capable of exactly calculating the transverse pressure gradient, but only at the leading shock front. And detailed numerical simulations in which the detonation reaction zone is resolved.

ROLE OF CONVECTION IN DETONATIONS

Figure 1 illustrates the different stages of reaction of a traditional detonation propagating in a heterogeneous explosive composed of energetic crystals and a binder. Two different pressure gradients develop in the reaction zone – macroscopic, from one control volume to the next, and microscopic, describing changes in pressure within the same control volume over length scales comparable to the particle size. Each pressure gradient drives the decomposition gas products in a different manner.

Upon crossing the shock, the explosive is compacted. As illustrated in Fig. 1a, the dissipated work is localized in a number of hot spots where ignition occurs. The resulting chemical decomposition *locally* raises the pressure at these hot spots, thus introducing within the same control volume a large number of microscopic pressure gradients, each pointing in a different direction. At each of these points, the difference in pressure forces the hot gas products to burn channels around and between particles, as illustrated in Fig. 1b. These channels eventually connect the isolated pockets of decomposition gas products together, thus partially deconsolidating the explosive, but more important, forming a network through which gases can travel macroscopic distances uninterrupted. When the decomposition products completely engulf the remaining solid fragments, the solid explosive becomes fluidized, as illustrated in Fig. 1c, and surface decomposition becomes the dominant reaction mechanism.

All the components within the control volume are subjected to the same macroscopic pressure gradient, but being lighter, the gas products acquire a higher velocity. The microscopic flows described above, driven in different directions by the microscopic pressure gradients within the control volume, do not add to a macroscopic flow with a net velocity component. But when driven by the macroscopic pressure gradient, the gas products can infiltrate through the network of open channels from one control volume into the next one downstream, as illustrated in Fig. 1c, same as convective burning in DDT. Eventually, due to the drag between the two phases, the remaining smaller fragments reach the same velocity as the gas products, and all 2-phase flow aspects cease. As illustrated in Fig. 1d, laminar surface decomposition then completes the reaction process, which in 1-D detonations and in detonations with slightly curved fronts has to end at the Chapman-Jouguet (CJ) surface.

By definition, in some sections of the reaction zone of a convective detonation, the hot gases from partially decomposed regions downstream infiltrate back to the shock and participate in the ignition process instead of solely depending on the shock-induced hot spots to start the reaction. In the traditional detonations described above, the macroscopic pressure gradients are pointed strictly downstream, the wrong direction for convection to contribute to ignition. But in highly curved detonations, the pressure gradient has a positive radial component. It can drive the gas products laterally, through pre-existing pores, shock or reaction-induced interstitial spaces, back to the front.

MODELING DETONATIONS IN SPATIALLY GRADED IDEAL EXPLOSIVES

A detailed account of the different aspects of

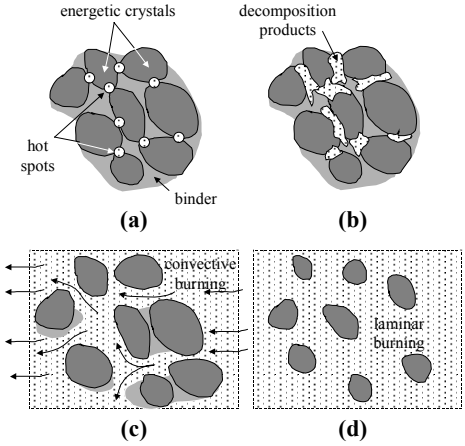

FIGURE 1. DIFFERENT STAGES OF REACTION IN A TRADITIONAL DETONATION

modeling detonations in spatially graded explosives is given in reference 1, but for clarity, a brief discussion of the important assumptions is included in this paper. The explosive charge is assumed pressed of two ideal explosives' energetic crystals - for example, PETN and TNT. The mass fraction of TNT, μ, and initial density distribution, ρ_o, can arbitrarily change with location $\mathbf{x}$ (x,y,z), but $\rho_o(\mathbf{x}) \le \mathrm{TMD}(\mathbf{x})$, where

$$\mathrm{TMD}(\mathbf{x}) = \frac{1}{\frac{1-\mu(\mathbf{x})}{\mathrm{TMD}_{\mathrm{PETN}}} + \frac{\mu(\mathbf{x})}{\mathrm{TMD}_{\mathrm{TNT}}}} \qquad (1)$$

The chemical energy stored in a unit mass of the explosive

$$e_o(\mathbf{x}) = [1-\mu(\mathbf{x})]\, e_o(\mathrm{PETN}) + \mu(\mathbf{x}) e_o(\mathrm{TNT}) \qquad (2)$$

In the numerical simulations $\rho_o(\mathbf{x})$ and $\mu(\mathbf{x})$ are convected with the flow in order to determine the initial values of ρ_o and μ at the location where the material originated.

TRANSVERSE PRESSURE GRADIENT AT THE SHOCK FRONT

The transverse pressure gradient in the reaction zone can be calculated without solving the PDE's describing the fluid flow, but only at the shock front. Figure 2 defines the nomenclature in a frame of reference moving with the wave. The flow is created by an axisymmetric curved detonation wave propagating steadily in the axial direction at velocity U. If the shock makes an angle θ with the z axis, the angular deflection of the flow δ can be determined from the trigonometric relations $U_n = U \sin\theta$ and $u_n = u \sin(\theta-\delta)$, where the subscript n denotes the velocity components normal to the front, and $U \cos\theta = u \cos(\theta-\delta)$, based on the conservation of momentum flux in the tangential direction, resulting in

$$\tan(\theta-\delta) = V \tan\theta \qquad (3)$$

where $V \equiv \rho_o/\rho = u_n/U_n$ by virtue of the conservation of mass flux across the shock.

Equation of Sate

As demonstrated in reference 1, if the reaction zone is infinitesimally thin, the detonation velocity is completely determined by the equation of state (EOS) of the decomposition products, and if the explosive is spatially graded, so does the shape of the front. This allows us to use a simple EOS for the unreacted solid explosive, here assumed described by a single (the same) Tait EOS, irrespective of the changes in local composition. The parameters b and γ in $-\nu(\partial p/\partial\nu)_S = b + \gamma p$ are assumed constants, independent of μ. The subscript S denotes an isentropic process and ν is the specific volume. Integrating, we get the pressure p and specific internal energy e on the isentrope:

$$p = B\left[\left(\frac{\rho}{\rho_o}\right)^{\gamma} - 1\right] \qquad (4a)$$

where $B \equiv b/\gamma$, and

$$e = e_o + \frac{p\nu - b(\nu_o - \nu)}{\gamma - 1} \qquad (4b)$$

In Eqs. 4a and 4b the initial (atmospheric) pressure was assumed negligible in comparison to the pressures generated by the detonation wave. The initial values ρ_o, $\nu_o \equiv 1/\rho_o$, and e_o change from point to point, as indicated by Eqs. 1 and 2.

Equation 4b can be rewritten as

$$p = b\left(\frac{\rho}{\rho_o} - 1\right) + \frac{\gamma - 1}{\nu}(e - e_o) \qquad (5)$$

in which the second term now appears as an incremental increase in pressure due to an increase in internal energy at constant volume, expressed in terms of Gruneisen $\Gamma \equiv \nu(\partial p/\partial e)_\nu = \gamma - 1$. For the constant energy process $e = e_o$, $(\partial p/\partial\nu)_e = (\partial p/\partial\nu)_S + p(\partial p/\partial e)_\nu = -(b+\gamma p)/\nu + \Gamma p/\nu$ gives $p = b(\rho/\rho_o - 1)$, the first term in Eq. 5. Instead of describing a process, Eq. 5 can now be considered a true EOS, $p(\rho,e)$, valid on and off the isentrope.

von Neumann State

Substituting $e - e_o = \tfrac{1}{2} p(\nu_o - \nu)$ in Eq. 5, we get the shock Hugoniot compatible with Tait EOS

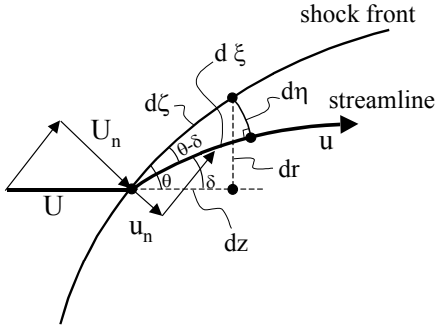

FIGURE 2. FLOW NEAR THE DETONATION FRONT

$$p = \frac{b\left(\frac{1-V}{V}\right)}{1-\frac{\gamma-1}{2}\left(\frac{1-V}{V}\right)} \qquad (6a)$$

But to calculate the transverse pressure gradient $\partial p/\partial \eta$ at the shock, p, V, and δ have to be expressed in terms of U, ρ_o, and θ. Intersecting the Rayleigh line $p = \rho_o U_n^2 (1-V)$ with the Hugoniot in Eq. 6a, we get

$$p = \frac{2b}{\gamma+1}\left(M_o^2 \sin^2\theta - 1\right) \qquad (6b)$$

and

$$V = \frac{\gamma-1}{\gamma+1} + \frac{2}{\gamma+1}\frac{1}{M_o^2 \sin^2\theta} \qquad (7)$$

The Mach number of the detonation wave $M_o \equiv U/c_o$, where the sound speed in the undisturbed explosive $c_o = \sqrt{(b/\rho_o)}$.

Transverse Pressure Gradient $\partial p/\partial \eta$

In terms of the curvilinear coordinates (ξ,η) illustrated in Fig. 2, aligned parallel and orthogonal to the streamlines,

$$\frac{\partial p}{\partial \eta} = \frac{\frac{\partial p}{\partial \xi}\cos(\theta-\delta) - \frac{dp}{d\zeta}}{\sin(\theta-\delta)} \qquad (8)$$

where ζ is the length measured along the shock front. Differentiating Eqs. 6b, 7, and 3, we get

$$\frac{\gamma+1}{2b M_o^2 \sin^2\theta}\frac{dp}{d\zeta} = -\frac{(\gamma+1)M_o^2 \sin^2\theta}{2}\frac{dV}{d\zeta} = \frac{d\ln \rho_o}{dr}\sin\theta + \frac{\sin 2\theta}{R \sin^2\theta} \qquad (9)$$

and

$$\frac{d\delta}{d\zeta} = \frac{1}{R}\left[1-\frac{V\cos^2(\theta-\delta)}{\cos^2\theta}\right] - \cos^2(\theta-\delta)\tan\theta\frac{dV}{d\zeta} \qquad (10a)$$

where R is the local radius of curvature of the front.

The change in pressure along the streamline[3]

$$\frac{\partial p}{\partial \xi} = -\rho u \frac{\sigma \dot{f} - u\frac{d\ln A}{d\xi}}{1-M^2} \qquad (11a)$$

σ df/dt is the thermicity. $\sigma \equiv (\partial v/\partial f)_{h,p}/v$, where the enthalpy $h \equiv e + pv$. df/dt is the rate of reaction, f being the burnt mass fraction. The local Mach number $M \equiv u/c$, where $c = \sqrt{(b+\gamma p)/\rho}$. The change in the cross sectional area of the infinitesimal, axisymmetric streamtube surrounding the streamline

$$\frac{d\ln A}{d\xi} = \frac{\sin\delta}{r} + \frac{\partial\delta}{\partial\eta} \qquad (11b)$$

where

$$\frac{\partial\delta}{\partial\eta} = \frac{1}{\sin(\theta-\delta)}\frac{d\delta}{d\zeta} \qquad (10b)$$

At the shock front where f = 0, $\sigma = v_g/v - 1$, where v_g is the specific volume that satisfies $p_g(v_g, h) = p$, p_g being the pressure of the incipient gas products.[4] If these are described by JWL EOS, A, B, R_1, R_2, and ω are determined by linearly interpolating between the corresponding JWL parameters for PETN and TNT.[1]

Effect of Diameter on $\partial p/\partial \eta$

$\partial p/\partial \eta$ at the shock front is plotted in Fig. 3 for 3 unconfined pressed PETN explosive charges, 2, 6, and 20 mm in diameter, assuming B = 39.3 kbar, γ = 4.1, resulting in $c_o \approx 3$ mm/μs, and U = 8 mm/μs. In all 3 cases a parabolic front profile obeying $z(r) = r^2/2R_o$ is assumed, but the radius of curvature at the axis R_o is calculated in each case based on the constraint that at the outer surface of unconfined (or lightly confined) charges, M = 1. For a given EOS (given composition), this constraint yields $\theta(r_o) \equiv \theta^*$ is a constant independent of the radius of the charge r_o. In Fig. 3, $\theta(r_o)$ is the same for all 3 cases; $\theta^* = 53.65^o$. But as the charge diameter is reduced the front becomes more curved. The transverse gradient $\partial p/\partial \eta$ increases, eventually becoming positive (pointing outward) throughout most of the domain when r_o = 1 mm. The effect of the reaction rate

$$\frac{df}{dt} = a(1-f)\left(\frac{p}{p^*}\right)^n \qquad (12)$$

on $\partial p/\partial \eta$ is also illustrated in Fig. 3. As the reaction rate increases, $\partial p/\partial \eta$ decreases. For all 3 cases shown in Fig. 3, p^* = 1 kbar.

Reducing the diameter is not, however, the only way of increasing the curvature of the front. As demonstrated by the sketch in Fig. 4, the front of a detonation propagating in a normal size charge can comprise a zone of locally high curvature, but still satisfy the same 2 constraints $\theta(0) \equiv 90^o$ and $\theta(r_o) \equiv \theta^*$ as the parabolic fronts in Fig. 3. For example, if the charge is radially graded whereby the core (r = 0 to r_1) is PETN, gradually changing to pure TNT in the outer layer (r_2 to r_o), then within the

transition layer (r_1 to r_2) the front will be highly curved. That is because for $r_1 >> d_c/2$ (for PETN, the critical diameter $d_c \approx 0.1$ mm), the detonation in the core will boost a nearly flat front for which $\theta \approx 90^o$, and will propagate at velocity $U \approx D_\infty \approx 8.3$ mm/μs, where D_∞ is the CJ detonation velocity as $d \rightarrow \infty$. However, because for TNT, $D_\infty \approx 6.9$ mm/μs, $\theta \approx \theta^* << 90^o$ throughout the outer layer. The change from $\theta = 90^o$ to θ^* will mostly occur within the transition layer, the narrower it is, the larger the local curvature of the detonation front. But if it is infinitesimally thin, wave reflections and refractions will be induced at the interface.

∂p/∂η in Radially Graded Explosive Charges

$\partial p/\partial \eta$ calculated using Eqs. 6 to 12 is plotted in Fig. 5a for a radially graded explosive pressed of PETN and TNT powders to TMD [$\rho_o(r)$ = TMD(r) given by Eq. 1] such that

$$\mu(r) = \frac{1 + tanh\left(3.8\ \beta\ \frac{r - \alpha\, r_o}{r_o}\right)}{2} \qquad (13)$$

The location and width of the transition layer are

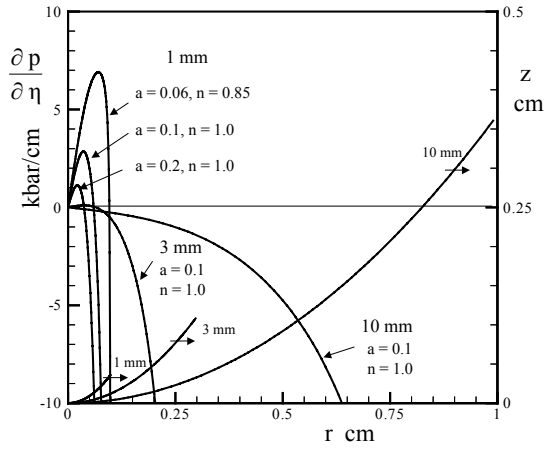

FIGURE 3. EFFECT OF DIAMETER ON TRANSVERSE PRESSURE GRADIENT

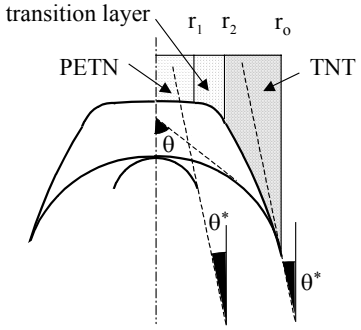

FIGURE 4. DETONATION FONT PROFILE IN A RADIALLY GRADED EXPLOSIVE

controlled by the parameters α and β, respectively.[5] The results shown in Fig. 5a are for α = ½ and β = 5. U = 8 mm/μs, B = 39.3 kbar, and γ = 4.1 yield θ^* = 53.83°. a = 0.06-0.2 μs^{-1}, n = 0.85-1, and p^* = 1 kbar, same as in Fig. 3, but instead of a pure PETN charge (μ = 0), the explosive is now radially graded, resulting in $\partial p/\partial \eta > 0$ for r ≈ 10 to 16 mm.

The front profile used to calculate these results was obtained by integrating an assumed curvature distribution,

$$\frac{1}{R} = \frac{\varepsilon}{R_c} + \frac{1-\varepsilon}{R_c}\left\{ tanh\left[3.8\,\kappa\,(r - r_1)\right] - tanh\left[3.8\,\kappa\,(r - r_2)\right]\right\} \qquad (14)$$

also shown in Fig. 5a for ε = 0.2, κ = 10, r_1 = 9 mm, and r_2 = 11 mm. ε and κ are adjustable parameters, but R_c controlling the radius of curvature in the transition layer is calculated such as to satisfy the constraint $M(r_o) = 1$. In the transition layer, the resulting streamlines are particularly divergent, as illustrated by the distribution of $d/nA/d\xi$.

Both Figs. 3 and 5a indicate that $\partial p/\partial \eta > 0$ in regions where the front is highly curved. But the effect of the rate of reaction in Fig. 5a appears to be opposite of that in Fig. 3. That is because for r ≈ 10 to 16 mm, σ < 0, as illustrated in Fig. 5b, ensuring that $\partial p/\partial \xi > 0$, as implied by Eq. 11a since $d/nA/d\xi > 0$, and $\partial p/\partial \eta > 0$, as implied by Eq. 8 since $dp/d\zeta < 0$. This situation does not usually arise, at least not in uniform explosives, because σ > 0 for a self-sustained detonation to propagate steadily.[4] But it is

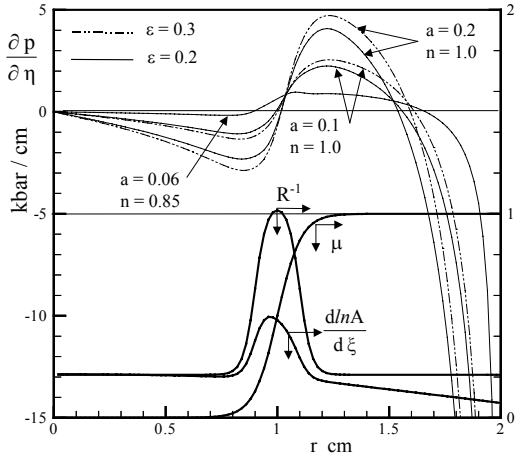

FIGURE 5A. ∂p/∂η IN A RADIALLY GRADED EXPLOSIVE FOR DIFFERENT REACTION RATES

possible in radially graded explosives because the shock in the transition layer is not self-sustained. It is driven by the detonation in the PETN core.

The shock Hugoniot described by Eq. 6a is plotted in Fig. 6 for B = 39.3 kbar and $\gamma = 4.1$. Shown as well are the Hugoniots for PETN and TNT detonation products. $p_g(\nu, h)$ are the corresponding pressure traces, but at the same enthalpy as the shock Hugoniot. For a pure explosive, whether it is PETN or TNT, $p_g(\nu, h) > p$ for all points on the shock Hugoniot located below the corresponding von Neumann state, yielding $\nu_g > \nu$ and $\sigma > 0$, where as explained above, ν_g is the volume that satisfies $p_g(\nu_g, h) = p$. But as demonstrated by Fig. 6, when PETN and TNT are combined in the same charge, the section of the shock Hugoniot located between the von Neumann state for PETN, and the point where it intersects the Hugoniot for TNT detonation products, is above $p_g(\nu, h)$ for TNT, resulting in $\nu_g < \nu$ and $\sigma < 0$.

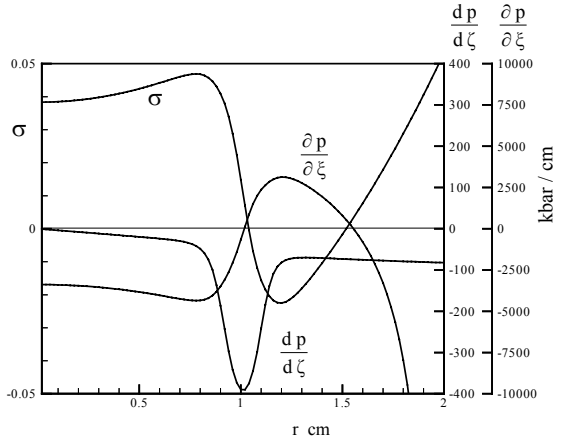

FIGURE 5B. NEGATIVE THERMICITY IN RADIALLY GRADED EXPLOSIVES

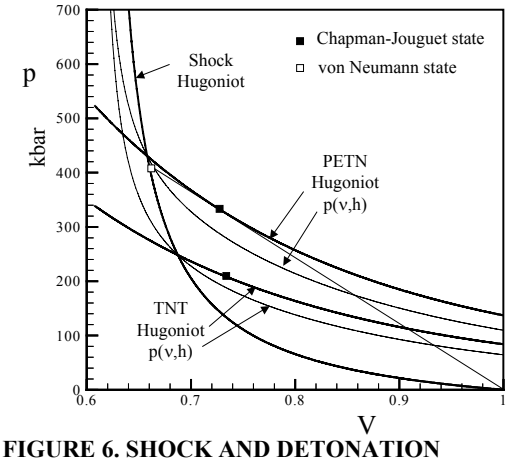

FIGURE 6. SHOCK AND DETONATION PRODUCTS HUGONIOTS

However, it is important to remember that the properties of the shock Hugoniot depend on the solid explosive EOS. For different values of B and γ, the points on the shock Hugoniot below the von Neumann state for PETN could have all fallen as well below $p_g(\nu, h)$ for both PETN and TNT, result-ing in $\sigma > 0$, always. Such is the case when B = 50 kbar and $\gamma = 2.0$.

SIMPLIFIED EOS FOR SOLID EXPLOSIVE

For the limited objectives of this paper, the EOS of the unreacted explosive can be further altered to simplify the numerical solution. We can neglect the difference between the possible thermodynamic paths and assume that the various states of the fragments of solid explosive within the reaction zone are located on a single process/path starting at the undisturbed state. Selecting the isentrope, the shock Hugoniot, or any other equivalent process to represent the change in the thermodynamic state is not as critical, but the EOS of the solid explosive has to obey some restrictions. The sound speed in the undisturbed explosive has to fall within the proper range with respect to the detonation velocity and the sound speed in the confinement. That is because detonations are supersonic waves, and the relative magnitude of the sound speed in the confinement affects the pattern of propagation - whether the detonation is leading the shock in the confinement or vice-versa. And the von Neumann pressure and density have to exceed the corresponding values at the CJ state.

The main benefit of neglecting the dependence of the different states of the unreacted explosive on the thermodynamic history is that in the numerical solution, we do not have to convect (keep track of) the individual volumes and internal energies of the solid explosive and/or detonation gas products separately. Pressure equilibrium is always assumed between the two phases. But at the end of a time-step, the pressure is determined based on instantaneous values, independently of the state of the unreacted explosive at the beginning of the time step, after the convection step, or any other point in time before equilibrium is established. The pressure in the reaction zone is determined by iteration.[1] The solid explosive is compressed or expanded along the isentrope until $p_g(\nu_g, e_g) = p(\nu)$, where $\nu_g = [\nu_{mix} - (1\text{-}f)\,\nu]/f$ and $e_g = [e_{mix} - (1\text{-}f)\,e(\nu)]/f$. $p(\nu)$ and $e(\nu)$ are given by Eqs. 4a and 4b.

$\partial p/\partial \eta$ Using Simplified EOS for Solid Explosive

If Eqs. 4a and 4b are used instead of Eq. 5, the

conservation equations describing the jump conditions across the shock become over-determined. If Eq. 4a is used to describe the shock Hugoniot instead of Eq. 6a, then $e-e_o = ½ p (v_o-v)$ cannot be satisfied. Equations 7 and 9 are replaced by

$$V = \left[\frac{1}{1+\gamma (1-V) M^2 \sin^2\theta} \right]^{1/\gamma} \qquad (15)$$

which as written, can be solved by using a point-iteration procedure starting at V = 0, and

$$\frac{B}{p+B} \frac{d\ln p}{d\zeta} = - \frac{\gamma B}{p} \frac{d\ln V}{d\zeta} = \frac{\frac{d\ln \rho_o}{dr} \sin\theta + \frac{\sin 2\theta}{R \sin^2\theta}}{\left(\frac{p}{B}+1\right) - V M^2 \sin^2\theta} \qquad (16)$$

$\partial p/\partial \eta$ calculated using the simplified EOS is plotted in Fig. 7 for U = 8 mm/μs, B = 22.3 kbar, γ = 7.15, yielding $\theta^* = 46.24^o$, a = 0.06-0.2 μs^{-1}, n = 0.85-1, p^* = 1 kbar, α = ½, β = 5, κ = 10, r_1 = 9 mm, and r_2 = 11 mm. $d\ln A/d\xi$ and R^{-1} are plotted for ε = 0.2. Again, $\partial p/\partial \eta > 0$ within a finite region near the transition layer.

NUMERICAL SIMULATIONS

The simplified EOS described above was implemented into GEMINI,[6] an Eulerian hydrocode based on the MUSCL scheme.[7] The high-order scheme is particularly important when resolving the effects of steep gradients in composition, as well as shocks and contact disconstinuities. To resolve the problem with a fixed grid, square cells 0.05 x 0.05 mm^2 were used throughout the explosive domain.

FIGURE 7. $\partial p/\partial \eta$ USING SIMPLIFIED EOS

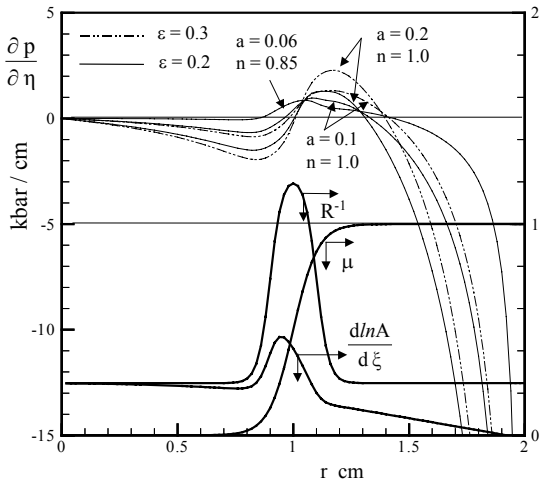

The pressure contours and streamlines generated by the underwater detonation of a 40 mm diameter charge, radially graded such that α = ½ and β = 5, are presented in Figs. 8a and 8b for B = 22.3 kbar, γ = 7.15, and 2 reaction rates corresponding to a = 0.06 μs^{-1}, n = 0.85 and a = 0.1 μs^{-1}, n = 1, resulting in 2 steady detonation waves propagating at U ≈ 7.9 and 8.2 mm/μs, and 2 different reaction zone thickness, 2.5 and 0.5 mm, respectively. Because as implied by Eq. 12, the burnt fraction increases to the limit f = 1 asymptotically, the contour f = 0.95 was arbitrarily selected instead to mark the end of the reaction zone.

In both cases, the gradual change in composition from PETN to TNT resulted in a detonation front that is highly curved in the region r ≈ 7.5 to 12.5 mm, but without introducing any appreciable reflection or refraction waves. Had the change been sudden, such as in layered explosives, strong reflection and refraction waves would have emanated from the shock at the point where it intersected the interface between adjacent layers.

In traditional detonations, and except at the outer surface, where for a lightly confined charge a Prandtl-Meyer expansion wave originates, the pressure contours in the vicinity of the front are parallel to the shock. As illustrated in Fig. 8a, this is mostly the case outside the transition layer. But in the region marked # 1, the pressure contours intersect the front at an accute angle that indicates that the pressure decreases as we approach the shock in a direction orthogonal to the streamlines, i.e., $\partial p/\partial \eta$ >

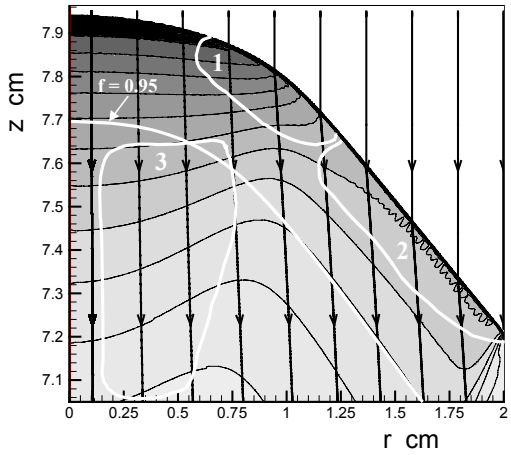

FIGURE 8A. PRESSURE CONTOURS AND STREAMLINES FOR a = 0.06 μs^{-1} AND n = 0.85

0. The opposite is true in region # 2, where the pressure increases as we move closer to the shock. Outside the immediate vicinity of the shock, $\partial p/\partial \eta > 0$ in region # 3 also. But this region is mostly outside the reaction zone. Although positive, the transverse pressure gradient in region # 3 cannot contribute to igniting the unreacted explosive coming through the section of the front bounding region # 2.

In the thin layer next to the front within region # 1 in Fig. 8b, the pressure also decreases as we move closer to the shock in a direction normal to the streamlines. But it is difficult in this case to depict the tight turns that the pressure contours make before they intersect the shock in this region because the reaction zone is only 0.5 mm thick.

DISCUSSION AND CONCLUSIONS

The reaction zone of detonation waves propagating in radially graded explosives is resolved using analytic techniques and numerical simulations. The results indicate that in regions where the change in composition causes a local increase in the curvature of the front and/or negative thermicity, the direction of the transverse pressure gradient is reversed. This can laterally drive the gas products from partially decomposed regions downstream back to the shock, which is necessary to demonstrate that convective detona-tions can occur in radially graded explosives, but not sufficient to prove that they will. That is because there are other factors essential to establishing convective detonations that could not be analyzed since they are outside the scope of the

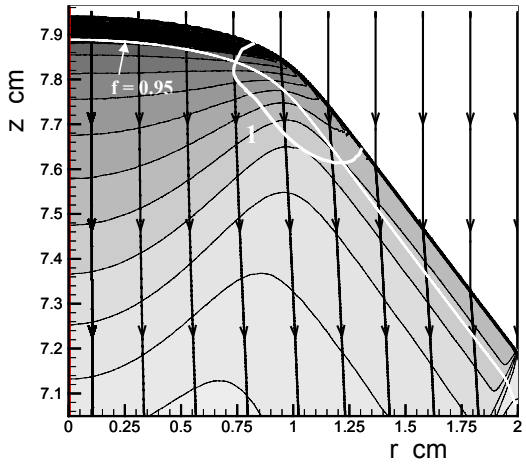

FIGURE 8B. PRESSURE CONTOURS AND STREAMLINES FOR a = 0.1 μs^{-1} AND n = 1.0

techniques used in this paper. For example, the depth of penetration of the gas products through the interstitial spaces depends on the damage induced by the shock, thus the fracture properties of the solid explosive. The contribution of the hot gases to igniting new materials that have already crossed the shock, but did not ignite yet, depends on the shock sensitivity of the explosive, ease of surface ignition, etc. The magnitude of the transverse pressure gradient cannot be determined to certainty because it depends on the EOS of the unreacted explosive and its rate of reaction, both routinely measured, but sensitive to factors such as binder content, chemical additives, etc.

On the other hand, the EOS of the detonation products is not as sensitive to the factors described above and is usually determined to a high degree of confidence using the cylinder test. Because the EOS of the consolidated solid explosive is independent of the EOS of the decomposition products, it may be always possible to find for the same energetic ingredients an explosive formulation the shock Hugoniot of which, favors the reversal of the direction of the transverse pressure gradient. For example, by yielding negative values for the thermi-city. Among others, these notions should increase our degree of confidence that convective detona-tions are possible in radially graded explosives.

REFERENCES

1. Guirguis, R., and Landsberg, A., "Structure of Detonation Waves in Stratified/Spatially-Graded Explosives," *Proceedings of the 19th JANNAF PSHS meeting*, 2000, CPIA, Columbia, MD.
2. Guirguis, R. and Landsberg, A., "Convective Detonations," *Proceedings of the 2001 APS Topical Conference on Shock Compression of Condensed Matter,* held in Atlamta, Georgia, June 24-29, 2001.
3. Fickett, W. and Davis, W. C., "Detonation," Sect. 5G, pp. 199-229, Univ. of California Press, 1979.
4. Guirguis, R. H., "1-D Detonability," *Proceedings of the 1995 APS Topical Conference on Shock Compression of Condensed Matter*, 377-380, 1995.
5. The constant 3.8 is a scaling factor for β; *tanh*(3.8) = 0.999.
6. Wardlaw, A., "Godunov Hydrocode Suite," IHTR 2088, NSWC, Indian Head, MD 20640, Sept. 1998.
7. Colella, P., "A Direct Eulerian MUSCL Scheme for Gasdynamics," *SIAM J., Sci. Stat. Comput.,* vol. 6, number 1, 104-117, 1985.